Materials Physics and Mechanics 44 (2020) 125-136 Received: July 29, 2019

CRYSTALLOGRAPHIC ORIENTATION, DELAY TIME AND MECHANICAL CONSTANTS INFLUENCE ON THERMAL FATIGUE STRENGTH OF SINGLE - CRYSTAL NICKEL SUPERALLOYS

A.V. Savikovskii[1*], A.S. Semenov[1], L.B. Getsov[2]

[1]Peter the Great St. Petersburg Polytechnic University, Polytechnicheskaya 29, St. Petersburg, 195251, Russia

[2]Joint-Stock Company "I.I. Polzunov Scientific and Development Association on Research and Design of Power Equipment", Polytechnicheskaya 24, St. Petersburg, 194021, Russia

*e-mail: savikovskii.artem@yandex.ru

Abstract. The influence of a delay time at the maximum temperature on the number of cycles for the macrocrack initiation for two thermal loading programs was investigated for two single-crystal nickel-based superalloys VIN3 and ZhS32. An analytic approximation of a delay time influence was proposed. Comparison of computational results and analytic formula on the base of constitutive equations with the experimental data was performed for considered single-crystal superalloys and showed a good accuracy. Influence of several mechanical constants of nickel alloy on thermal fatigue strength is presented and discussed. The influence of crystallographic orientation of the corset sample on the thermal fatigue durability with delay times for various thermal loading programs and different single-crystal nickel superalloys was investigated.

Keywords: thermal fatigue, single-crystal nickel-based superalloy, deformation criterion, corset sample, crystallographic orientation, finite element modeling, analytic approximation

1. Introduction

Single-crystal nickel-based superalloys [1] are used for production of gas turbine engines (GTE) [2]. These materials have a pronounced anisotropy and temperature dependence of properties. Cracking in the turbine blades is caused often by thermal fatigue [3,4]. For investigation of thermal fatigue durability under a wide range of temperatures with and without delay times the experiments are carried out on different types of samples, including corset (plane) specimen [3] on the installation developed in NPO CKTI [5] (see Fig. 1). Fixed in axial direction by means of two bolts with a massive foundation the corset sample (see Fig. 2) is heated periodically by passing electric current through it. The fixing of sample under heating leads to the high stress level and inelastic strain appearance. The FE simulation is required for the computation of inhomogeneous stress and inelastic strain fields.

The aims of the study are: (I) to study numerically a stress-strain state of the sample during cyclic heating and cooling due to its clamping, (II) to study systematically the effect of delay at maximum temperature on the thermal fatigue durability on the base of the four-term deformation criterion [6-8] of thermal-fatigue failure for single crystal superalloys using the results of finite element (FE) simulation of full-scale experiments and results of analytical formulae and (III) to study systematically the effect of crystallographic orientation on the thermal fatigue durability. The results of simulation and their verification are obtained for different single-crystal nickel-based superalloys: VIN3 and ZhS32.

http://dx.doi.org/10.18720/MPM.4412020_15

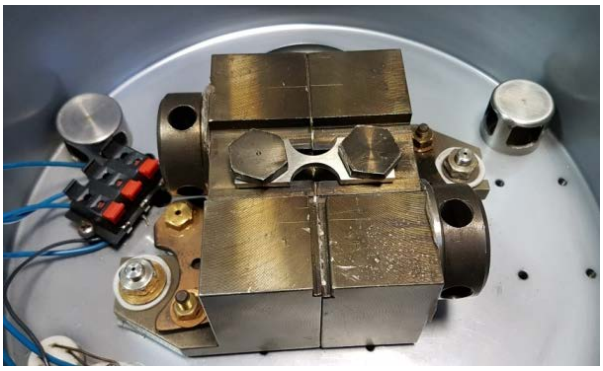

Fig. 1. Testing setup for thermal fatigue experiments

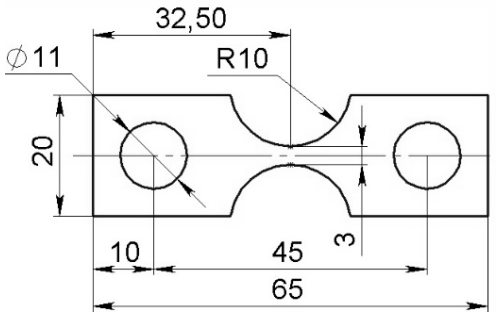

Fig. 2. Geometrical parameters of the corset sample

2. Results of thermo-elasto-visco-plastic analysis

The axial fixing of the corset specimen under heating leads to the high axial stress and inelastic strain appearance. The numerical simulation is required for the computation of inhomogeneous stress and inelastic strain fields in sample. Modeling and simulation of inelastic cyclic deformation of corset samples has been performed by means of the FE programs ANSYS and PANTOCRATOR [9], which allows to apply the micromechanical (microstructural, crystallographic, physical) models of plasticity and creep for single crystals [10-14]. The micromechanical plasticity model accounting 12 octahedral slip systems with lateral and nonlinear kinematic hardening [10,15] is used in the FE computation for the simulation of single crystal superalloy behavior under cyclic loading. The Norton power-type law is used to describe creep properties.

Modeling of inelastic deformation in the corset samples has been performed with taking into account of the temperature dependence of all material properties, anisotropy of mechanical properties of single-crystal sample, inhomogeneous nonstationary temperature field, mechanical contacts between bolt and the specimen, between specimen and foundation, friction between the contact surfaces, temperature expansion in the specimen. The viscous properties are taken into account because of high temperature despite of a quick time of heating and cooling of the corset samples.

The two FE formulations for the thermo-mechanical problem have been considered:

• FE model with taking into account equipment;

• FE model without taking into account equipment (simplified formulation [16] for the sample only).

Using of the second formulation provides significant saving computational time due to reduction in the number of degrees of freedom and refusal to solve a contact problem. It is very actual for the numerous multivariant computations for different regimes of loading and the crystallographic orientations. The validity of the simplified formulation is based on the comparison with the results of full-scale formulation (with taking into account equipment), as

well as on the comparison with the relative displacements of two markers measured in experiments.

In the general case there is no symmetry in the problem (Fig. 3a) due to anisotropy of mechanical properties of single crystal sample. However in the important for practice case of [001] crystallographic orientation of sample the symmetry in respect to planes *xz* and *yz* (see Fig. 3a) can be introduced. Equipment and bolts are modeled by linear elastic material (steel), and for the sample elasto-visco–plastic model of material is used. The problem is solved in a three-dimensional quasi-static formulation. As boundary conditions the symmetry conditions are set: zero displacements on the *y*-axis on the *xz* plane and zero displacements on the *x*-axis on the *yz* plane. On the lower side of the equipment zero displacements along the *x* and *z* axes are set. On the bolt cap the pressure of 100 MPa has been applied that is equivalent to the tightening force of the bolt. The temperature boundary conditions are set from the experimental data at maximum and minimum temperature with linear interpolation in time. The results of finite element heat conduction simulations [17] consistent with experimental temperature field distributions. The mechanical properties for the alloy VIN3 are taken from the paper [18] and for the alloy ZHS32 from [19] are summarized in Tables 1 and 2. The mechanical properties of bolts are taken for pearlitic steel [20].

Table 1. Mechanical properties of VIN3 used in simulations [18]

T	°C	20	500	700	900	1000	1050
E_{001}	MPa	126000	110000	104000	89000	80000	75000
ν	-	0.39	0.41	0.42	0.42	0.425	0.428
α	1/K	$1.21\cdot10^{-5}$	$1.33\cdot10^{-5}$	$1.4\cdot10^{-5}$	$1.5\cdot10^{-5}$	$1.57\cdot10^{-5}$	$1.6\cdot10^{-5}$
σ_y^{001}	MPa	555	800	930	910	645	540
n	-	3	3	3	3	3	3
A	$\text{MPa}^{-n}\text{s}^{-1}$	$1\cdot10^{-27}$	$8\cdot10^{-17}$	$2.3\cdot10^{-15}$	$6.5\cdot10^{-14}$	$3.5\cdot10^{-13}$	$8\cdot10^{-13}$

Table 2. Mechanical properties of ZHS32 used in simulations [19]

T	°C	20	500	700	900	1000	1050
E_{001}	MPa	137000	110000	105000	99800	94800	92300
ν	-	0.395	0.4248	0.4284	0.4317	0.4347	0.4361
α	1/K	$1.24\cdot10^{-5}$	$1.6\cdot10^{-5}$	$1.7\cdot10^{-5}$	$1.81\cdot10^{-5}$	$2.22\cdot10^{-5}$	$2.42\cdot10^{-5}$
σ_y^{001}	MPa	919	904	901	895	670	580
n	-	8	8	8	8	8	8
A	$\text{MPa}^{-n}\text{s}^{-1}$	$1\cdot10^{-42}$	$2.5\cdot10^{-31}$	$8.5\cdot10^{-30}$	$2\cdot10^{-28}$	$6\cdot10^{-27}$	$7\cdot10^{-26}$

In simplified formulation of the problem (see Fig. 3b) we consider only the sample without equipment, in which zero displacements on the symmetry planes *xz* and *yz* are set, the outer face of the sample parallel to the symmetry plane *xz* was fixed in the direction of the axis *x*. To exclude solid body motions, a number of points on this face are also fixed in the direction of the *y* and *z* axes.

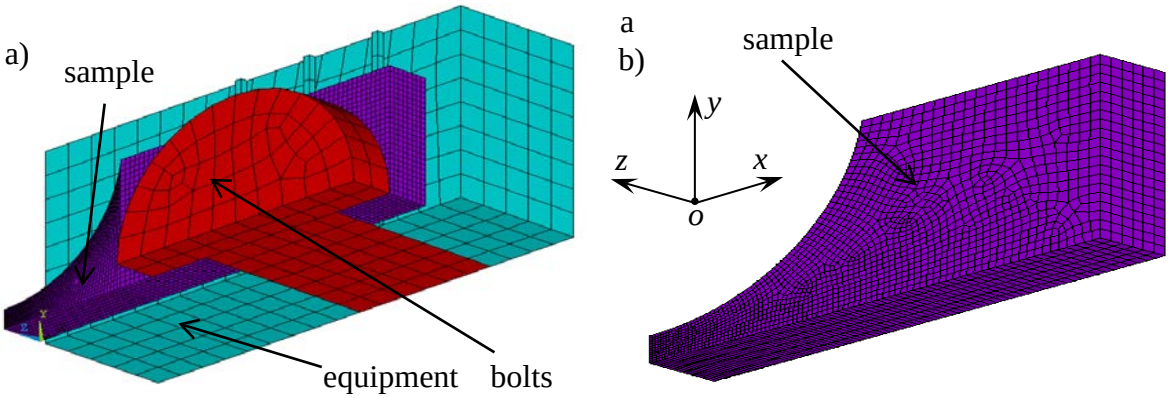

Fig. 3. FE models of the corset sample for thermo-elasto-visco-plastic problem solution:
a) model (¼ due to symmetry) with taking into account of equipment,
b) simplified model (¼ due to symmetry) without taking into account of equipment

Figure 4 shows distributions of plastic strain intensity field for two nickel superalloys and three different temperature modes after 7 cycles (for VIN3 the effective length of the sample is 42 mm, for ZHS32 is 50 mm) [17] obtained with using the FE model (¼ due to symmetry) without taking into account equipment (Fig. 3b).

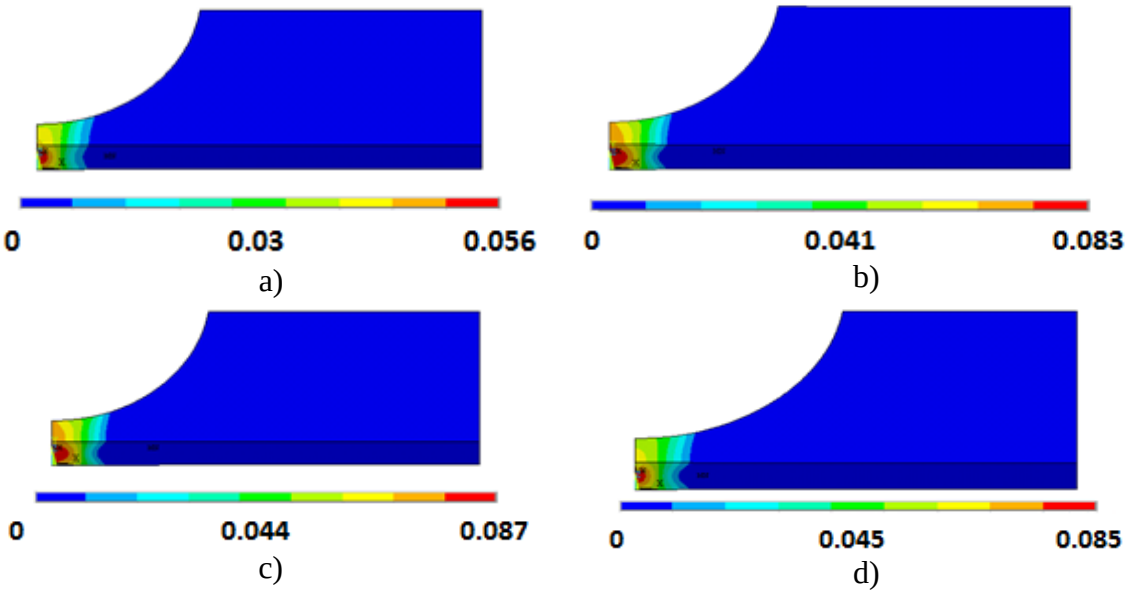

Fig. 4. Plastic strain intensity field distributions in the corset sample after 7 cycles for:
a) superalloy ZhS32, loading regime 150÷900°C;
b) superalloy ZhS32, loading regime 500÷1050°C;
c) superalloy ZhS32, loading regime 700÷1050°C;
d) superalloy VIN3, loading regime 500÷1050°C

Table 3 shows the equivalent (effective) length of the sample for the simplified formulation for different alloys, which has been found by the comparison with full model using the condition of equality of the inelastic strain ranges. In the FE simulations with acceptable engineering accuracy can be used the value 40 mm. Effective length takes into account the compliance of equipment and its variation in considered range has no appreciable on the results.

Table 3. The equivalent length of the corset sample for different alloys

VIN3	ZhS32
38 – 46 mm	40 – 52 mm

3. Influence of the delay on the thermal fatigue durability

FE computations are carried out for a part of a corset sample (simplified FE model with effective length of sample equal 40 mm, see Fig. 3b). The temperature fields are set from the experimental data at maximum and minimum temperature cycle phase with using linear interpolation in time.

The influence of the delay at maximum temperature on the number of cycles to the formation of macrocrack is analyzed in the range from 1 min to 1 hour for the cyclic loading regimes with:

- maximum temperature of 1050°C and minimum temperature of 700°C;
- maximum temperature of 1050°C and minimum temperature of 500°C;
- maximum temperature of 1000°C and minimum temperature of 500°C;
- maximum temperature of 900°C and minimum temperature of 150°C.

The heating time in the cycle is 10s, the cooling time is 16s for VIN3. The heating times in the cycle are 15s, 15s, 10s, 25s, the cooling times are 15s, 15s, 14s, 75s for ZhS32. The mechanical properties for the alloy VIN3 were taken from the paper [18] and for the alloy ZhS32 from [19] (see also Tables 1 and 2).

The problem is solved in a quasi-static 3-dimensional formulation. The FE model is shown in Fig. 3b. The boundary conditions are zero displacements in the direction of the *x*-axis on two side faces of the sample with the normal along the *x*-axis. To exclude rigid body motions, a number of points on these faces in the direction of the *y* and *z* axes are also fixed.

Temperature evolutions in central point of sample with and without delay for loading regimes 700÷1050°C, 500÷1050°C, 250÷1000°C and 150÷900°C are presented schematically in Fig. 5.

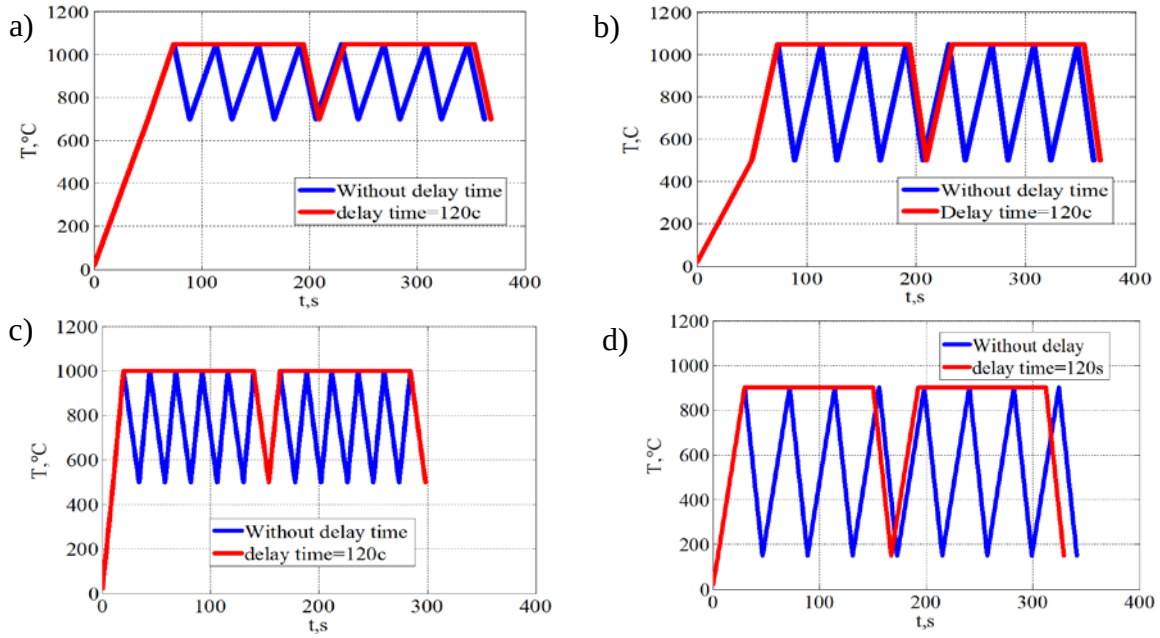

Fig. 5. Schematic presentations of temperature evolutions in central point of sample for loading regimes with and without delay time:
a) 700÷1050°C; b) 500÷1050°C; c) 500÷1000°C and d) 150÷900°C

Damage calculation and estimation of the number of cycles for the macrocrack initiation are made on the basis of four-term deformation criterion [6-8,14]:

$$D=\sum_{i=1}^{N}\frac{(\Delta\varepsilon_{eqi}^{p})^{k}}{C_1(T)}+\sum_{i=1}^{N}\frac{(\Delta\varepsilon_{eqi}^{c})^{m}}{C_2(T)}+\max_{0\le t\le t_{\max}}\frac{\varepsilon_{eq}^{p}}{\varepsilon_r^{p}(T)}+\max_{0\le t\le t_{\max}}\frac{\varepsilon_{eq}^{c}}{\varepsilon_r^{c}(T)}, \quad (1)$$

where the first term takes into account the range of plastic strain within the cycle, the second term deals with the range of creep strain within the cycle, the third term is unilaterally accumulated plastic strain (ratcheting), the fourth term is unilaterally accumulated creep strain. The number of cycles to initiate macrocrack N is determined from the condition $D = 1$. The equivalent strain for single crystal is defined by maximum shear strain in the slip system with normal to the slip plane $\mathbf{n}_{\{111\}}$ and the slip direction $\mathbf{l}_{\langle 011\rangle}$:

$$\varepsilon_{eq}=\mathbf{n}_{\{111\}}\cdot\boldsymbol{\varepsilon}\cdot\mathbf{l}_{\langle 011\rangle}. \quad (2)$$

Usually it takes in (1) the values of constants: $k=2$, $m=\frac{5}{4}$, $C_1=\left(\varepsilon_r^{p}\right)^{k}$, $C_2=\left(\frac{3}{4}\varepsilon_r^{c}\right)^{m}$, where ε_r^{p} and ε_r^{c} are ultimate strains of plasticity and creep under uniaxial tension. In the FE computations the values of ultimate strains $\varepsilon_r^{p}=\varepsilon_r^{c}=18\%$ are used the same for all considered alloys. Improvement of the prediction accuracy of the delay time influence on durability can be achieved by the refinement of the constant strains ε_r^{p} on the basis of data without delay.

Analytic approximation [21] is offered to enter for describing of delay time influence on thermal fatigue durability. The additive strain decomposition [22] is used for the small strain case under uniaxial relaxation at constant temperature and total strain:

$$\varepsilon=\varepsilon_e+\varepsilon_p+\varepsilon_c+\varepsilon_t=\varepsilon_0, \quad (3)$$

where ε is the total strain, $\varepsilon_e=\frac{\sigma}{E}$ is the elastic strain, ε_p is the plastic strain, ε_c is the creep strain and ε_t is the thermal strain, ε_0 is constant. Differentiating (3) and using $\dot{\varepsilon}_p=\frac{\dot{\sigma}}{H}$ (where H is the hardening modulus), Norton law $\dot{\varepsilon}_c=A\sigma^{n}$ with taking into account notation $E_T=\left(E^{-1}+H^{-1}\right)^{-1}$ for the tangent modulus it can be obtained equation:

$$\sigma^{-n}\dot{\sigma}=-AE_T. \quad (4)$$

Using result of integration of differential equation (4) from t_0 to t for $\sigma(t)$ in the relation $\dot{\varepsilon}_c=A\sigma^{n}$ allow us to introduce differential equation for creep strain:

$$\dot{\varepsilon}_c=A\left[\sigma_0^{1-n}+(n-1)AE_T(t-t_0)\right]^{\frac{n}{1-n}}. \quad (5)$$

Result of integration of (5) from t_0 to t has the form:

$$\Delta\varepsilon_c=-\frac{1}{E_T}\left\{\frac{1}{\left[\sigma_0^{1-n}+(n-1)AE_T(t-t_0)\right]^{\frac{1}{1-n}}}-\frac{1}{(\sigma_0^{1-n})^{\frac{1}{1-n}}}\right\}, \quad (6)$$

which can be rewritten as following:

$$\Delta\varepsilon_c=\frac{\sigma_0}{E_T}\left\{1-\left[1+\frac{(n-1)E_T}{\sigma_0}A\sigma_0^{n-1}(t-t_0)\right]^{-\frac{1}{1-n}}\right\}. \quad (7)$$

Using simplified two-term deformation criterion with taking into account creep strain terms:

$$\frac{\varepsilon^{c}_{accumul}}{\varepsilon_r}+N\left(\frac{\Delta\varepsilon_c}{\varepsilon_r}\right)^{m}=1, \tag{8}$$

where ε_r is the ultimate strain of creep under uniaxial tension, N is the number of cycles of macrocrack initiation we obtain:

$$N=\left(\frac{\varepsilon_r}{\frac{\sigma_0}{E_T}\left\{1-\left[1+\frac{(n-1)E_T}{\sigma_0}A\sigma_0^{\,n-1}t_{delay}\right]^{\frac{1}{1-n}}\right\}}\right)^{m}\cdot\left(1-\frac{\varepsilon^{c}_{accumul}}{\varepsilon_r}\right). \tag{9}$$

In the simulations we use: $\sigma_0=(\alpha_{20-T_{max}}\cdot T_{max}-\alpha_{20-T_{\min}}\cdot T_{min})\cdot E_T\cdot 0.9$, $\alpha_{20-T_{max}}$ and $\alpha_{20-T_{\min}}$ are the coefficients of linear thermal expansion, $E_T=9.48\cdot10^4/9.98\cdot10^4$ MPa, $A=2\cdot10^{-28}/6\cdot10^{-27}$ MPa^{-n}s^{-1}, $\varepsilon_r=0.18$ for alloy ZhS32, $A=8\cdot10^{-13}$ MPa^{-n}s^{-1}, $\varepsilon_r=0.18$ for alloy VIN3. Multiplier $1-\frac{\varepsilon^{c}_{accumul}}{\varepsilon_r}$ is picking up to correlate one point with experiment.

Comparison of results of FE simulations, experiments and analytical approximation (9) concerning the effect of the delay time at the maximum temperature on the thermal fatigue durability for single-crystal superalloys VIN3 and ZhS32 for four temperature modes is given in Fig. 6.

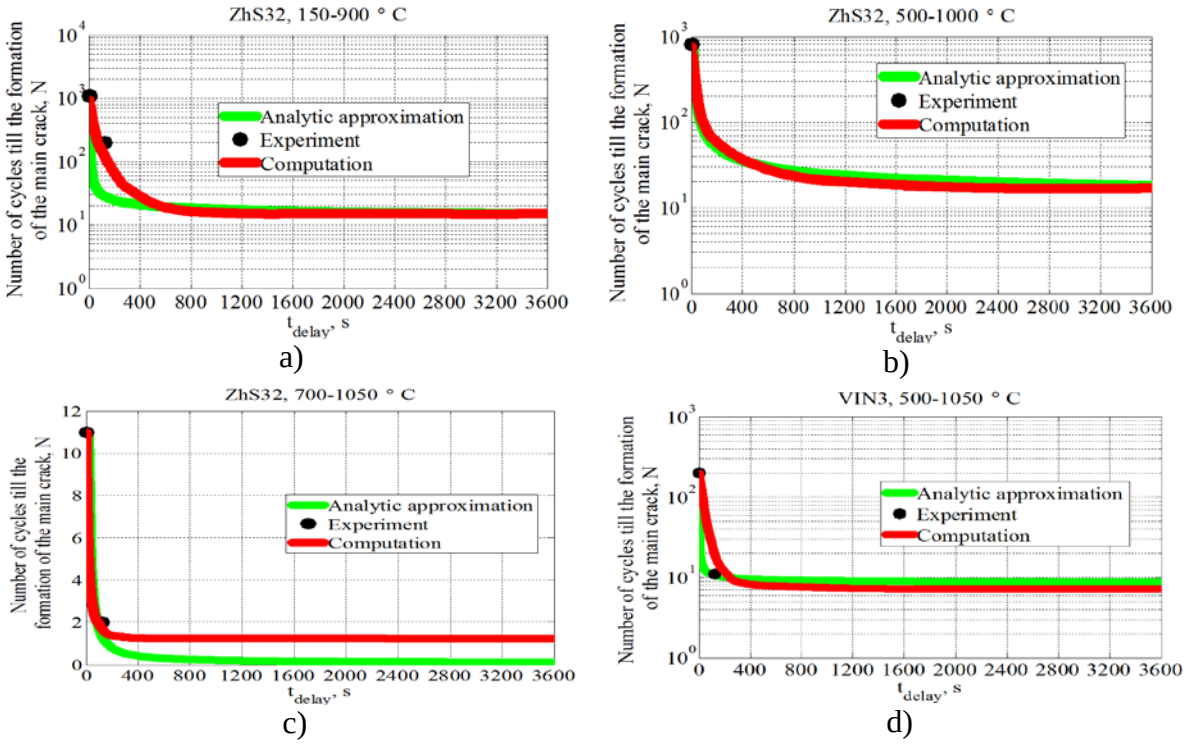

Fig. 6. Comparison of results of FE simulations, analytical approximation and experimental data for alloys: a) ZhS32, loading regime 150÷900°C, heating time is 25 s, cooling time is 75 s; b) ZhS32, loading regime 500÷1000°C, heating time is 10 s, cooling time is 14 s; c) ZhS32, loading regime 700÷1050°C, heating time is 15 s, cooling time is 15 s; d)VIN3, loading regime 500÷1050°C, heating time is 10 s, cooling time is 16 s

Figure 7 shows creep strain intensity field distributions for nickel superalloys ZhS32 and VIN3 in case without delay time and with delay time 5 minutes after 10 cycles.

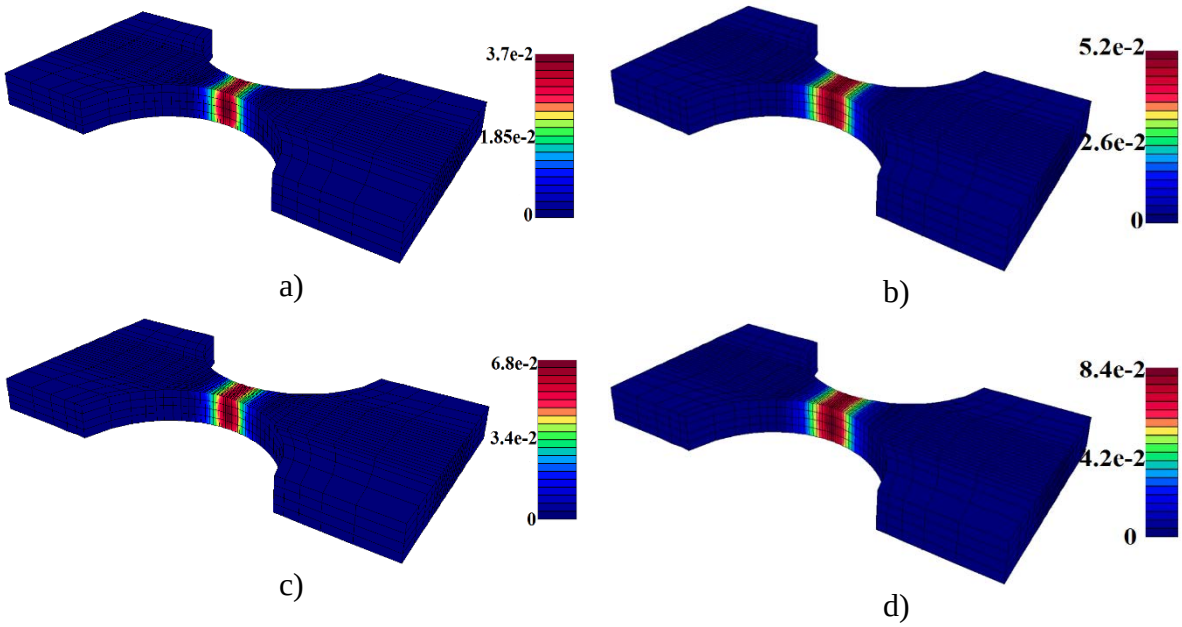

Fig. 7. Creep strain distributions:
a) ZhS32, loading regime 150÷900°C, without delay time; b) VIN3, loading regime 500÷1050°C, without delay time; c) ZhS32, loading regime 150÷900°C, with delay time 5 minutes; d) VIN3, loading regime 150÷900°C, with delay time 5 minutes

Several material parameters appearing in the analytic formula (9) and calculations such as A, n and ε_r are more complicated to obtain and to find in open sources. Influence of these constants on thermal fatigue durability for nickel alloys ZhS32 and VIN3 and two temperature loading regimes is investigated. The results of parametrical analysis are presented in Fig. 8 with varied values of A, n and ε_r.

Numerical simulations show that parameters n and ε_r influence stronger, then parameter A on thermal fatigue durability.

In gas turbine blades direction of mechanical, thermal and other loadings may not the same as crystallographic orientation (CGO) of single-crystal blade. CGO of gas turbine blades and the samples have an effect on creep rate and thermal fatigue durability. Influence of CGO on thermal fatigue strength is important to predict behavior and damage of single-crystal alloys. Influence of crystallographic orientation (CGO) on thermal fatigue strength for superalloys ZhS32 and VIN3 for four temperature modes is presented in Fig. 9.

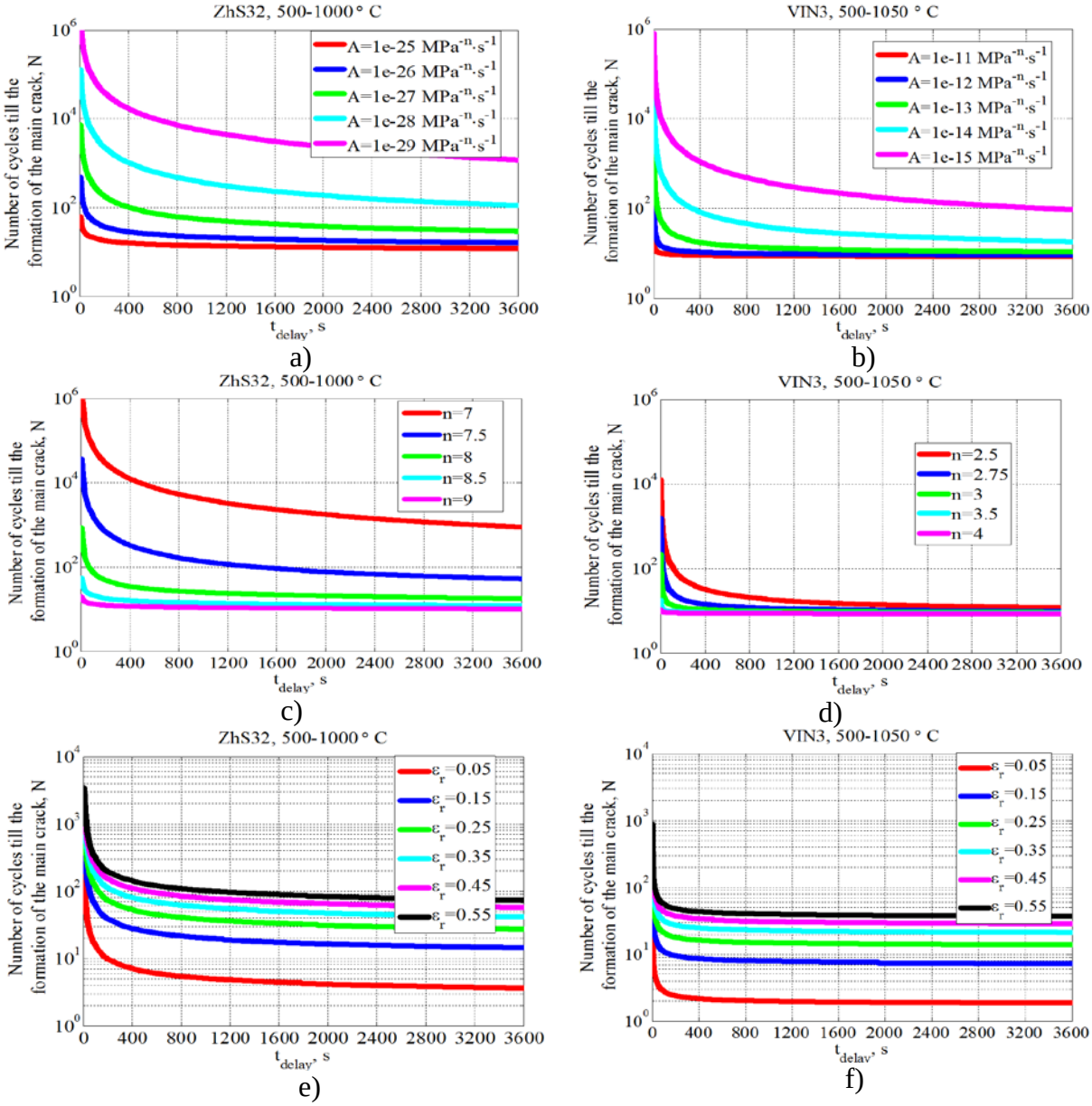

Fig. 8. Influence of material parameters of nickel-based alloys on thermal fatigue durability:

a) Influence of parameter *A*, ZhS32, loading regime 500÷1000°C, $\varepsilon_r = 0.18$, $n = 8$;

b) Influence of parameter *A*, VIN3, loading regime 500÷1050°C, $\varepsilon_r = 0.18$, $n = 3$;

c) Influence of parameter *n*, ZhS32,loading regime 500÷1050°, $\varepsilon_r = 0.18, A = 6 \cdot 10^{-27}$ MPa^{-n}s^{-1}

d) Influence of parameter *n*,VIN3, loading regime 500÷1050, $\varepsilon_r = 0.18, A = 8 \cdot 10^{-13}$ MPa^{-n}s^{-1};

e) Influence of parameter ε_r, ZhS32, loading regime 500÷1050°C, $n = 8$, $A = 6 \cdot 10^{-27}$ MPa^{-n}s^{-1};

f) Influence of parameter ε_r, VIN3, loading regime 500÷1050°C, $n = 3$, $A = 8 \cdot 10^{-13}$ MPa^{-n}s^{-1}

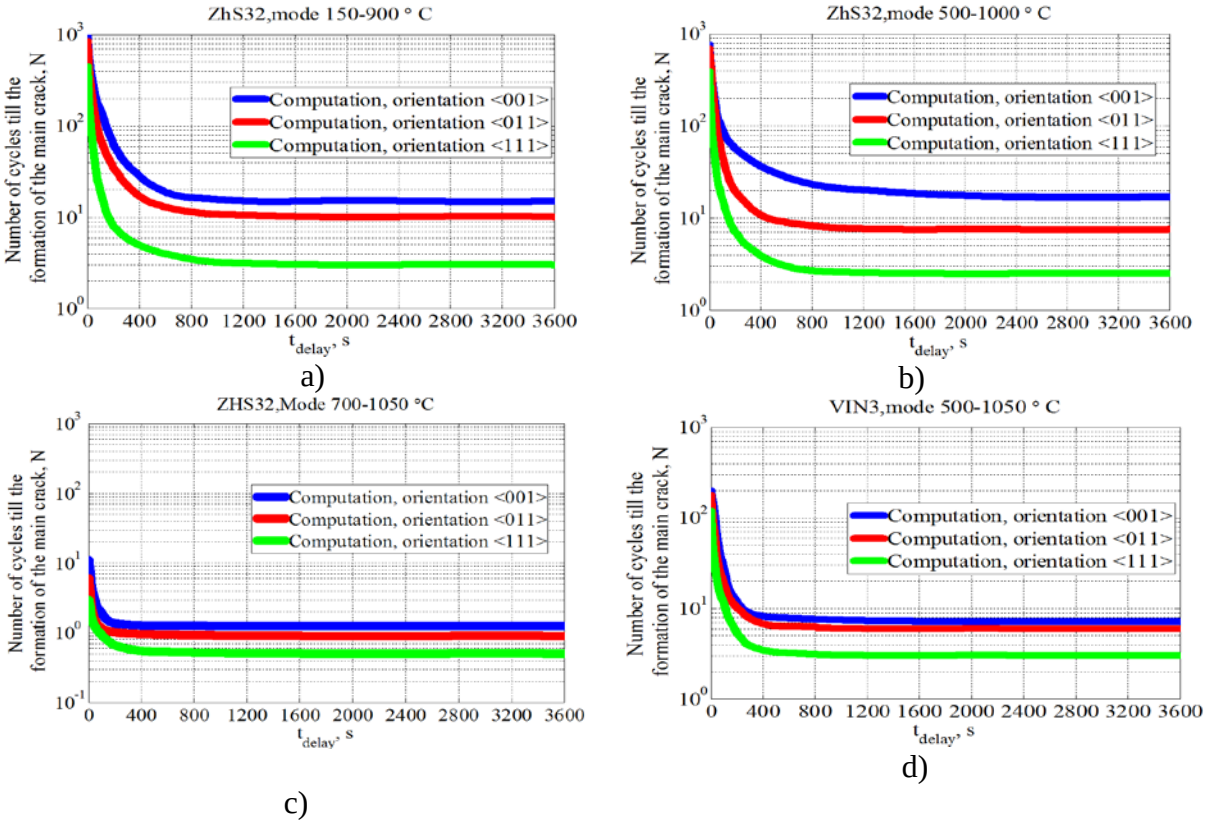

Fig. 9. Influence of crystallographic orientation on thermal fatigue durability for single-crystal nickel-based superalloys:
a) ZhS32, T = 150÷900ºC, heating time is 25s, cooling time is 75s, $\varepsilon_r = 0.18$;
b) ZhS32, T = 500÷1000ºC, heating time is 10s, cooling time is 14s, $\varepsilon_r = 0.18$;
c) ZhS32, T = 700÷1050ºC, heating time is 15s, cooling time is 15s, $\varepsilon_r = 0.18$;
d) VIN3, T = 500÷1050ºC, heating time is 10s, cooling time is 16s, $\varepsilon_r = 0.18$

The reason of the superiority of thermal fatigue durability for samples with CGO <001> over CGO <011> and <111> is associated with lower values of Young's modulus for CGO <001> ($E_{\langle 111\rangle} / E_{\langle 001\rangle} = 2.4$, $E_{\langle 111\rangle} / E_{\langle 011\rangle} = 1.4$ at 1000ºC).

4. Conclusions

Computational results of thermal fatigue durability showed a good agreement with the experiments, which suggests that finite-element modeling and analytical approximation (9) in combination with deformation criterion (1) can be used to predict thermal-fatigue strength of single-crystal nickel-based superalloys.

Investigation of material parameters influence show that creep exponent n and tensile rupture strain ε_r affect more stronger that creep parameter A on thermal fatigue durability of single-crystal nickel based superalloys. Constants n and ε_r should be more accurately obtained from experimental data.

The thermal fatigue durability of corset samples from superalloys ZhS32 and VIN3 with CGO <001> exceeds the thermal fatigue durabilities of CGO <011> and <111> (Fig. 9) for all considered loading programs and alloys.

Comparison analysis of superalloys ZhS32 and VIN3 showed that superalloy ZhS32 has thermal fatigue strength higher than superalloy VIN3 for the same considered loading program.

Acknowledgments. The reported study was supported by RFBR according to the research project №19-08-01252.

References

[1] Shalin RE, Svetlov IL, Kachanov EB, Toloraiya VN, Gavrilin OS. *Single crystals of nickel heat-resistant alloys.* M.: Mashinostroenie; 1997.
[2] Kablov EN, Golubovsky ER. *Heat resistance of nickel-based alloys*. M.: Mashinostroenie; 1998.
[3] Dulnev RA, Kotov PI. *Thermal fatigue.* M.: Mashinostroenie; 1980.
[4] Getsov LB, Dobina NI, Rybnikov AI, Semenov AS, Staroselskii A, Tumanov NV. Thermal fatigue resistance of a monocrystalline alloy. *Strength of materials*. 2008;40(5): 538-551.
[5] Getsov LB. *Materials and strength of gas turbine parts.* Rybinsk: Gazoturbinnye Tekhnologii; 2010.
[6] Getsov LB, Semenov AS. Criteria of fracture of polycrystalline and single crystal materials under thermal cyclic loading. *Proceedings of CKTI*. 2009;296: 83-91.
[7] Semenov AS, Getsov LB. Thermal fatigue fracture criteria of single crystal heat-resistant alloys and methods for identification of their parameters. *Strength of Materials*. 2014;46(1): 38-48.
[8] Getsov LB, Semenov AS, Staroselsky A. A failure criterion for single-crystal superalloys during thermocyclic loading. *Materials and technology*. 2008;42: 3-12.
[9] Semenov AS. PANTOCRATOR – finite-element program specialized on the solution of non-linear problems of solid body mechanics. *Proc. of the V-th International. Conf. "Scientific and engineering problems of reliability and service life of structures and methods of their decision"*. SPb.: Izd-vo SPbGPU; 2003: 466-480.
[10] Cailletaud GA. Micromechanical approach to inelastic behaviour of metals. *Int. J. Plast.* 1991;8: 55-73.
[11] Asaro RJ. Crystal plasticity. *Journal of Applied Mechanics.* 1983;50(4b): 921-934.
[12] Trusov PV, Volegov PS, Kondratyev NS. *The physical theory of plasticity.* Perm; 2013. (In Russian)
[13] Semenov AS. Identification of anisotropy parameters of phenomenological plasticity criterion for single crystals on the basis of micromechanical model. Scientific and technical sheets SPbGPU. *Physical and mathematical Sciences.* 2014;2(194): 15-29.
[14] Semenov AS, Grishchenko AI, Kolotnikov ME, Getsov LB. Finite-element analysis of thermal fatigue of gas turbine blades. *Vestnik UGATU (scientific journal of Ufa State Aviation Technical University)*, 2019;23(1): 70-81.
[15] Melnikov BE, Semenov AS, Semenov SG. Multimodel analysis of elastoplastic deformation of materials and structures. Current state. *Trudi CNII im. Acad. A. N. Krylova*. 2010;(53): 85-92.
[16] May S, Semenov AS. Modeling of inelastic cyclic deformation of monocrystalline specimens. *Proc. of the XXXIX week of science of SPbPU*. 2010;5: 73-74.
[17] Savikovskii AV, Semenov AS, Getsov LB. Coupled thermo-electro-mechanical modeling of thermal fatigue of single-crystal corset samples. *Materials Physics and Mechanics.* 2019;3(42): 296-310.
[18] Semenov SG, Getsov LB, Semenov AS, Petrushin NV, Ospennikova OG, Zhivushkin AA. The issue of enhancing resource capabilities of nozzle blades of gas turbine engines through the use of new single crystal alloy. *Journal of Machinery Manufacture and Reliability.* 2016;4: 30-38.

[19] Getsov LB, Semenov AS, Tikhomirova EA, Rybnikov AI. Thermocyclic and static failure criteria for single crystal superalloys of gas turbine blades. *Materials and technology.* 2014;2: 255-260.
[20] Maslenkov SB, Maslenkova EA. *Steels and alloys for high temperatures.* Moscow: Metallurgia; 1991.
[21] Savikovskii A, Semenov A, Getsov L. Analysis of crystallographic orientation influence on thermal fatigue with delay of the single-crystal corset sample by means of thermo-elasto-visco-plastic finite-element modeling. *Matec Web of Conferences*. 2018;245.
[22] Palmov VA, Stain E. Decomposition of final elastic-plastic deformation into elastic and plastic components. *Bulletin of Perm national research Polytechnic University*. 2001;9: 110-126.